Water Research X 7 (2020) 100050

Contents lists available at ScienceDirect

Water Research X

journal homepage: https://www.journals.elsevier.com/water-research-x

Transport and retention of artificial and real wastewater particles inside a bed of settled aerobic granular sludge assessed applying magnetic resonance imaging

Florian Ranzinger [a, **], Maximilian Matern [a], Manuel Layer [b], Gisela Guthausen [a, c], Michael Wagner [a, d], Nicolas Derlon [b], Harald Horn [a, e, *]

[a] Engler-Bunte-Institut, Water Chemistry and Water Technology, Karlsruhe Institute of Technology, Engler-Bunte-Ring 9, 76131, Karlsruhe, Germany
[b] Eawag, Swiss Federal Institute of Aquatic Science and Technology, Department of Process Engineering, CH-8600, Dübendorf, Switzerland
[c] Institute for Mechanical Process Engineering and Mechanics, Karlsruhe Institute of Technology, Adenauerring 20b, 76131, Karlsruhe, Germany
[d] Karlsruhe Institute of Technology, Institute of Biological Interfaces (IBG-1), Hermann-von-Helmholtz-Platz 1, 76344, Eggenstein-Leopoldshafen, Germany
[e] DVGW Research Laboratories, Water Chemistry and Water Technology, Engler-Bunte-Ring 9, 76131 Karlsruhe, Germany

ARTICLE INFO

Article history:
Received 13 September 2019
Received in revised form
14 January 2020
Accepted 16 March 2020
Available online 6 April 2020

Keywords:
Aerobic granular sludge
Particulate organic matter
Magnetic resonance imaging
Anaerobic feeding phase
Colloid
Wastewater particle
Hydrolysis

ABSTRACT

The removal or degradation of particulate organic matter is a crucial part in biological wastewater treatment. This is even more valid with respect to aerobic granular sludge and the impact of particulate organic matter on the formation and stability of the entire granulation process. Before the organic part of the particulate matter can be hydrolyzed and finally degraded by the microorganism, the particles have to be transported towards and retained within the granulated biomass. The understanding of these processes is currently very limited. Thus, the present study aimed at visualizing the transport of particulate organic matter into and through an aerobic granular sludge bed. Magnetic Resonance Imaging (MRI) was successfully applied to resolve the different fractions of a granular sludge bed over time and space. Quantification and merging of 3D data sets allowed for a clear determination of the particle distribution within the granular sludge bed. Dextran coated super paramagnetic iron oxide nanoparticles (SPIONs, d_p = 38 ±10 nm) served as model particles for colloidal particles. Microcrystalline cellulose particles (d_p = 1–20 μm) tagged with paramagnetic iron oxide were applied as a reference for toilet paper, which is a major fraction of particulate matter in domestic wastewater. The results were supplemented by the use of real wastewater particles with a size fraction between 28 and 100 μm. Colloidal SPIONs distributed evenly over the granular sludge bed penetrating the granules up to 300 μm. Rinsing the granular sludge bed proved their immobilization. Microcrystalline cellulose and real wastewater particles in the micrometer range accumulated in the void space between settled granules. An almost full retention of the wastewater particles was observed within the first 20 mm of the granular sludge bed. Moreover, the formation of particle layers indicates that most of the micrometer-sized particles are not attached to the biomass and remain mobile. Consequently, these particles are released into the bulk phase when the granulated sludge bed is resuspended.

1. Introduction

Within the last decade aerobic granular sludge systems for municipal wastewater treatment have proved to be economically competitive compared to the activated sludge systems (Giesen et al., 2013; Pronk et al., 2015b). By now, around 50 aerobic granular sludge reactors have been set into operation in full scale for the treatment of wastewater (HaskoningDHV, 2020; Li et al., 2014). Despite these full scale plants only little is known about the granulation process during municipal wastewater treatment as well as the factors causing low or high effluent concentrations of particulate organic matter (Derlon et al., 2016; Rocktäschel et al., 2015; Wagner et al., 2015; Wilén et al., 2018).

Around 50% of the chemical oxygen demand in municipal wastewater are dedicated to particulate organic matter. The latter

* Corresponding author. Engler-Bunte-Institut, Water Chemistry and Water Technology, Karlsruhe Institute of Technology, Engler-Bunte-Ring 9, 76131, Karlsruhe, Germany.
** Corresponding author.
E-mail addresses: Florian.Ranzinger@kit.edu (F. Ranzinger), Harald.Horn@kit.edu (H. Horn).

https://doi.org/10.1016/j.wroa.2020.100050

represents a crucial carbon source in municipal wastewater treatment (Orhon and Çokgör, 1997). Particulate organic matter has to undergo hydrolysis before it can be metabolized to carbon dioxide and new biomass by the microorganisms. The removal of particulate organic matter can be divided into 4 steps: (I) external transport to the biofilm surface, (II) attachment of the particles, (III) hydrolysis of particulate organic matter and release of hydrolytic products, (IV) uptake of these products by microorganisms (Boltz and Motta, 2007; Li et al., 2018). Theories about the removal of particulate organic matter in granular sludge reactors typically assume that it attaches/adsorbs at the granule surface during the feeding phase (De Kreuk et al., 2010; Pronk et al., 2015a). Overall, the degradation of particulate organic matter takes several days (Benneouala et al., 2017). Thus, attachment is a prerequisite to ensure that particulate organic matter can serve as a carbon source for aerobic granular sludge systems and is not washed out with the effluent.

To understand how particulate organic matter behaves within a bed of settled granules during anaerobic feeding, imaging techniques might be applied. Imaging techniques such as confocal laser scanning microscopy (CLSM), optical coherence tomography (OCT), and micro-computer tomography (μ-CT) are either limited by their penetration depth or by exposing microorganisms to potentially harmful radiation (Adav et al., 2008; Bouma, 2001; Li et al., 2018; Peszynska et al., 2016). Magnetic Resonance Imaging (MRI) is a powerful and widely applied tool in biofilm research (Herrling et al., 2019; Neu et al., 2010). MRI is a non-destructive *in situ* method with a spatial resolution down to a few tenth of μm. MRI offers the spatial investigation of the distribution of NMR active nuclei (commonly ^{1}H), relaxation times, diffusional and advective transport. An image contrast between water and biofilm is generated by their difference in the so-called longitudinal (T_1) and transverse (T_2) relaxation times (Manz et al., 2003; Seymour et al., 2004). The image contrast depends on the biofilm properties, i.e., its compactness and chemical composition. So far, MRI studies mainly focused on water diffusion and distribution in biofilms, transport and fate of heavy metals, trace metals, macromolecular substances and nanoparticles (Bartacek et al., 2016; Herrling et al., 2017; Phoenix et al., 2008; Ramanan et al., 2013; Ranzinger et al., 2016). In addition, MRI can be applied to resolve the dynamics of the water distribution and structure of the biofilm. Several studies explored biofilm development, its impact on fluid flow, biomass distribution and shape as well as cohesive and adhesive strength in tube reactors or porous media (Graf von der Schulenburg et al., 2008; Manz et al., 2003; Seymour et al., 2004; Wagner et al., 2010).

The current study aims at exploiting the capabilities of MRI in order to assess the fate of particulate organic matter during the anaerobic feeding phase of a granular sludge bed. To our knowledge, mass transport studies have been limited to single granules and/or did not resolve an entire granular sludge bed. The main objectives of this study were thus: (i) to demonstrate the feasibility and applicability of MRI for the (structural) characterization of granular sludge beds, (ii) to investigate the transport, loading and retention behavior of particulate organic matter within a bed of settled granules and (iii) to demonstrate the dependence of the retention mechanism on the size of particulate organic matter. Super paramagnetic iron oxide nanoparticles (SPIONs, $d_p = 38 \pm 10$ nm) have been applied which resemble the colloidal fraction of particulate organic matter. The results are supplemented by the investigation of artificial microcrystalline cellulose particles (MCPs, $d_p = 1–20$ μm) and real wastewater particles (WWPs, $d_p = 28–100$ μm) as models for particulate organic matter in the micrometer range.

2. Material and methods

2.1. Aerobic granular sludge

Aerobic granular sludge was taken from a lab-scale sequencing batch reactor (SBR) at Eawag. Samples were sieved to separate flocs from aerobic granules ($d \geq 0.63$ mm). The granule size allowed for a sufficient resolution of the voids between the granules. The granules had a smooth surface and a typical size range of 1–2 mm. Granules were send from Eawag (Dübendorf, Switzerland) to Karlsruhe (Germany): Approx. 200 mL of granular sludge were filled in a bottle and covered to the top with tap water. The bottle was send on ice in a styrofoam box. The maximum delivery time was two days. The first MRI experiments were started immediately after sample arrival. However, granular sludge samples were stored in the fridge (4 °C) not longer than five days in case the experiments had to be repeated. The latter could occur due to air bubbles or incorrect packing of the granules.

2.2. Preparation and characterization of particulate organic matter

Colloidal particles (SPIONs)

Superparamagnetic iron oxide nanoparticles (SPIONs) with a diameter d_p of 38 ±10 nm were utilized as reference for colloidal particles resembling the colloidal fraction of particulate organic matter, (nanomag®-D-spio; Micromod Partikeltechnologie GmbH, Rostock, Germany). SPIONs consist of iron oxide cores covered by an organic dextran matrix. Large macromolecules consisting of dextran have been successfully applied in hydrolysis experiments before (Confer and Logan, 1997). SPIONs have a zeta potential close to zero. Further, the particles showed no signs of agglomeration or sedimentation. The iron oxide cores serve as paramagnetic tagging causing fluctuating disturbances of the magnetic field. Hence, mainly transverse relaxation is enhanced creating predominantly a T_2 contrast. Information about the applied particle concentration and loading is given in Table 1. A detailed characterization of these particles is given in Cuny et al. (2015).

Microcrystalline cellulose particles (MCPs) as model particulate organic matter

Cellulose is a major fraction of particulate organic matter in domestic wastewater as it originates from toilet paper (Ruiken et al., 2013). A dispersion of the base product (Alfa Aesar, Thermo Fisher Scientific GmbH, Karlsruhe, Germany) was sonicated and wet sieved to collect a size fraction between 1 and 20 μm. For paramagnetic tagging, MCPs have been suspended in a 50 g/L ferrous sulphate solution under anoxic conditions. After draining, the iron(II) saturated microcrystalline cellulose particles were dried at room temperature over night to allow for a complete oxidation of the often diamagnetic iron(II) to paramagnetic iron(III). No mobilization of iron(III) ions was recognized later on.

Real wastewater particles (WWPs)

Primary effluent wastewater of the pilot-scale wastewater treatment plant at Eawag, Dübendorf (Switzerland) was collected to extract real WWPs. After centrifuging (3000 rpm, 5 min) and decanting settled particles were collected and freeze-dried. Before conducting the experiment, the freeze-dried particles were suspended in ultrapure water, homogenized and wet sieved. A size fraction between 28 and 100 μm was further used.

Table 1
Experimental conditions for the experiments. To meet the requirements for MRI measurements, sample design and conditions differ from full- or lab-scale application. Changes between experiments are explained in chapter 2.4.

	Experiment 1	Experiment 2	Experiment 3
Applied particles	colloidal particles (SPIONs)	microcrystalline cellulose particles (MCPs)	real wastewater particles (WWPs)
paramagnetically tagged?	yes	yes	no
mean particle diameter/size range	38 ±10 nm	1–20 μm	28–100 μm
average flow velocity	0.78 m/h	0.78 m/h	0.39 m/h
flow direction	top to bottom	bottom to top	bottom to top
dry mass of particles applied during the experiment	13 mg	139 mg	155 mg
concentration	73.1 mg/L	1.0 g/L	4.7 g/L
particle load:			
applied volume | duration |	37 mL | 37 min |	80 mL | 80 min |	24 mL | 48 min |
dry mass of particles applied	2.7 mg	80 g	113 g
additional particle load:			
applied volume | duration |	140 mL | 140 min |	59 mL | 59 min |	9 mL | 18 min |
dry mass of particles applied	10.28 mg	59 g	42.3 g

2.3. Experimental setup and procedure

A small sample design was necessary, to meet imaging requirements (sufficient signal-to-noise ratio). The authors are aware that due to the small column diameter wall effects have a larger impact on the process compared to commonly applied pilot and full scale aerobic granular sludge reactors.

A schematic of the experimental setup is presented in Fig. 1. The aerobic granules were placed inside a glass column with an inner diameter of 14 mm and a length of 100 mm. The height of the bed of settled granular sludge was approximately 50 mm. 2 cm space were given at each end of the column to distribute the flow before reaching the granular sludge bed. At the bottom glass spheres with a diameter of 2 mm stabilized the granular sludge bed. An O-ring and a mesh (size 0.7 mm, fabric) were positioned in between to separate the granules from the glass spheres. Both beds were wet packed to avoid air entrapment. The glass column was installed into the 200 MHz spectrometer and connected to a peristaltic pump (Ismatec, IPC, IDEX Health and Science GmbH, Wertheim, Germany) via polytetrafluoroethylene capillaries (inner diameter: 0.75 mm; Duratec Analysentechnik GmbH, Hockenheim, Germany).

The granular sludge bed was initially rinsed with tap water for 60 min with a volumetric flow rate of 1 mL/min, corresponding to a flow velocity of 0.78 m/h. The particles were pumped through the column during two loading phases (see Table 1). In between the flow was turned off for image acquisition. The particle suspension (feed) was positioned on a magnetic stirrer being continuously mixed to avoid particle sedimentation. As channeling occurred at average velocities higher than 1 m/h, the particle concentration was adjusted to ensure a moderate experiment duration.

2.4. Adjusted parameters between experimental runs

The artificial particles (SPIONs and MCPs) were paramagnetic tagged. Paramagnetic tagging strongly enhances image contrast via paramagnetic relaxation enhancement. Untreated particulate organic matter does not significantly alter the MRI signal, unless it appears in a large concentration and geometric extensions e.g. in form of particle layers. The occurrence of particle layers in Experiment 2, lead to the conclusion that paramagnetic relaxation enhancement is not necessary for micrometer sized particles in large concentrations. Thus, no paramagnetic relaxation enhancement was conducted in Experiment 3. In addition, a larger minimum particle diameter has been chosen for the WWPs to conclusively neglect penetration into the biofilm matrix.

As channeling occurred at average velocities higher than 1 m/h, the particle concentration was adjusted to ensure a moderate experiment duration. In addition, the average flow velocity was adjusted in Experiment 3 due to the channeling event in Experiment 2. In general, high concentrations of particles in relation to biomass were necessary to allow for a clear detection of the transport behavior and differentiation of particles and granular sludge (e.g., signal-to-noise ratio).

Flow direction and field of view were changed for Experiment 1 due to the aim of highlighting the granular sludge bed in contact with the bulk interface. Due to their particle size SPIONs are staying suspended for weeks without any signs of settling.

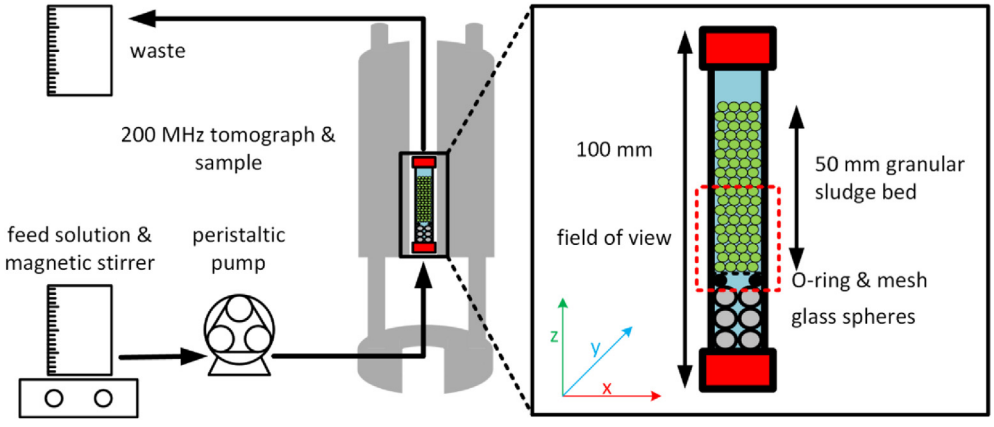

Fig. 1. Experimental setup. MRI images were acquired along the first 22.5 mm of the granular sludge bed, according to the flow direction.

2.5. Magnetic resonance imaging

The experiments were performed on a 200 MHz nuclear magnetic resonance spectrometer (Bruker Avance HDIII 200 SWB, Bruker BioSpin GmbH, Rheinstetten, Germany). The superconducting magnet has a vertical bore of 150 mm and a magnetic-flux density B_0 of 4.7 T. A 25 mm birdcage of the MICWB 40 series was used. Gradients up to 1.5 T/m were available in all spatial directions (x, y, z). Multi-slice multi-echo imaging (MSME) was performed in 2D and 3D as provided within Paravision 6.0.1 (Bruker BioSpin GmbH, Rheinstetten, Germany). A signal-to-noise study revealed that a combination of T_1- and T_2-weighting is the most convenient. T_1-weighted images favor the so called longitudinal relaxation differences, while simultaneously, but to a smaller extent transverse relaxation is occurring. Vice versa, the same applies for T_2-weighted images. T_1-weighted images were used to differentiate between granules and the bulk liquid. T_2-weighted images were acquired to supplementary locate the added particles within the bed of settled granules. Data acquisition parameters are listed in Table 2.

2.6. Data analysis and visualization

Data analysis was performed within Matlab R2018b (MathWorks, Nattick, MA, US) using home-written scripts and Avizo 9.4 (Thermo Fisher Scientific, Waltham, Masssachusetts, USA). Graphical illustrations of the data analysis are provided in the supporting information. Briefly, the 3D datasets recorded at the end of each experiment have been segmented via interactive thresholding. In the T_1-weighted images the shell of the granules showed high signal intensity and appeared bright. These signals were used to separate the granules from the background (e.g., bulk water phase). From T_2-weighted images the dark appearing particles were extracted. The resulting binary datasets were combined, and an artificial color allocation was given to differentiate between void space (black), granules (green) and particles (yellow). In addition, granules and particles were assigned to the fraction of "granule + particle" (white) in case of spatially overlapping signals (co-localization, see Fig. S1). It has to be noticed, that the void space includes all voxels which have not been assigned to granules or particles during thresholding. In particular, these are interpreted as water filled pores and channels as well as the interior of granules (confer T_1-weighted images in Fig. S1).

Quantification has been achieved as follows: The volumetric fractions of each class have been determined for a region of interest in 3D. As the wastewater particles were also visualized (T_1-weighted images), image analysis was adapted to quantify the fractions of granules, particles and void spaces correctly within the limitations of the approach (see supporting information S2).

3. Results

3.1. Experiment 1: Behavior of colloidal particles (SPIONs)

The aim of this experiment was to visualize and quantify the interaction of SPIONs in the bulk phase and the granular sludge bed. A set of MRI images shows the behavior of SPIONs in the granular sludge bed (Fig. 2). In Fig. 2A the T_1-weighted images show the structure of the granular sludge bed. Bulk liquid phase and granules can be distinguished based on their respective T_1-relaxation times. After applying the particle load, SPIONs were distributed within the pores of the granular sludge bed as visible in Fig. 2A after step II. SPIONs enhance the relaxation of the liquid phase. The result is a brighter appearing liquid phase and a declined contrast between granules and liquid phase in T_1-weighted images immediately after the SPION injection (compare steps I and II in Fig. 2A). However, the T_2-weighted images are more sensitive for the detection of SPIONs due to the inherent relaxivities of these SPIONs (Cuny et al., 2015). In T_2-weighted images (Fig. 2B, step II) the enhanced relaxation causes the low signal intensity of the liquid phase. In contrast to the initial image shown in Fig. 2B (step I), the liquid phase can be distinguished from the granules in T_2-weighted images.

To study the interaction of the SPIONs with and within the granular sludge bed driven by diffusion, flow was stopped. After 16 h without flow the pore space within the granular sludge bed appears bright in T2 weighted images (Fig. 2B, step III), which correlates to a low SPION concentration. The sorption of the colloidal particles to the granule surface is visible as a "ring" of low intensity in the T_2-weighted images in Fig. 2B (step III). In relation to the intensity of the granular sludge bed, the dark appearing bulk liquid phase above the granular sludge bed (see Fig. 2B, step III) indicates a relatively high concentration of SPIONs. Without applied flow the SPIONs were not deeply entering the granular sludge bed, as no concentration gradient within the granular sludge bed is observed (Fig. 2B, step III z = 0–14 mm). An additional particle load was reestablishing the concentration of SPIONs within the pore space of the granular sludge bed (compare Fig. 2A and B, steps II and IV). By rinsing the granular sludge bed (see Fig. 2, step V), mobile particles were removed. The T_2-weighted image in Fig. 2B (step V) shows residual SPIONs immobilized at the granule surface (see "dark" rings). The liquid above and within the pore space exhibit a similar signal intensity compared to the initial state indicating a low SPION concentration in the bulk liquid (compare Fig. 2A, steps I and V).

3.2. Experiment 2: Behavior of microcrystalline cellulose particles (MCPs)

The set of T_1- and T_2-weighted MRI images in Fig. 3 illustrates the behavior of MCPs (d_p = 1–20 μm) in the granular sludge bed.

Table 2
MRI data acquisition parameters. If not mentioned differently, the parameter values apply to both 2D and 3D measurements.

	T_1-weighted	T_2-weighted
Repetition time (T_R)	500 ms	2000 ms
Echo time (τ_E)	5 ms	2D: 30 ms, 3D: 35 ms
Averages	2D: 16, 3D: 2	2D: 4, 3D: 1
Image matrix size	2D: 192 × 128	
2D: *zx*-plane	3D: 192 × 128 × 128	
Field of view	2D: 22.5 mm × 15 mm	
2D: *zx*-plane	3D: 22.5 mm × 15 mm × 15 mm	
Resolution	117 μm isotropic in 3D, in plane in 2D	
Slice thickness	1 mm (only 2D)	
Slice gap	2 mm (only 2D)	
Scan duration	2D: 17 min, 3D: 4.5 h	2D: 17 min, 3D: 9 h

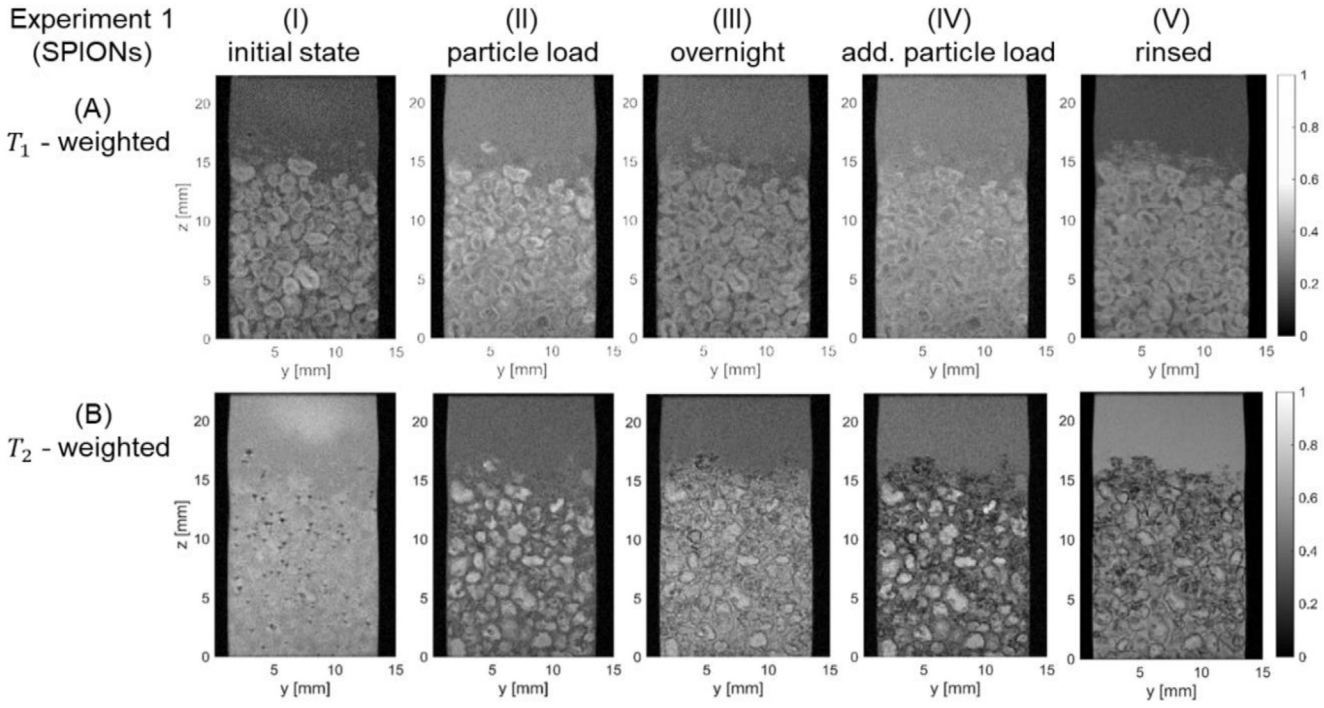

Fig. 2. 2D MRI images (cross-sections) showing the distribution and sorption of SPIONs within the granular sludge bed. T_1-weighted images (A) allow for a differentiation between granules and water filled pore space, while T_2-weighted images (B) are more sensitive to SPION concentrations (e.g. particle load). The presence of SPIONs in the liquid enhances mainly T_2 relaxation, but markedly affects also the T_1 contrast. Sorption of SPIONs to granules is indicated as their surface becomes visible in terms of "dark" rings in T_2-weighted images.

The formation of a channel through the granule bed can be observed on Fig. 3A steps I to III at $y = 10–15$ mm. MCPs are not recognizable in the T_1-weighted images.

After the initial particle load MCPs accumulated below the granular sludge bed which is indicated by the darker regions in Fig. 3B (step II; $z = 0–3$ mm). Further accumulations of MCPs are visible along the channel at $y = 10–15$ mm (see Fig. 3B, step II). In detail, MCPs are found at the granule surfaces or in void spaces situated next to the channel. Nevertheless, the major part of the granular sludge bed is free from MCPs (bright regions remaining in step II compared to step I in Fig. 3B).

After the additional particle injection (see Fig. 3B, step III) further particle accumulation filled void space next to the channel and partially the channel itself, while no (additional) particles distributed over the rest of the granular sludge bed. The development of a preferential flow path at $y = 10–15$ mm through the granular sludge bed was further confirmed by measuring flow (data not shown).

3.3. Experiment 3: Behavior of real wastewater particles (WWPs)

Fig. 4 illustrates the behavior of real WWPs ($d_p = 28–100$ μm) inside the granular sludge bed. To avoid immediate channeling as observed during the experiment with MCPs (see section 3.2 above), the average flow velocity was lowered to 0.39 m/h.

Compared to the particles applied in the first two experiments (SPIONs, MCPs), WWPs caused an additional image contrast in predominantly T_1-weighted images (see Fig. 4A, steps II and III). WWPs appear brighter than the granules. The WWPs appear also more inhomogeneous in terms of signal intensity and are surrounded by some susceptibility artifacts (black dots in bright layer Fig. 4A, steps II and III). The T_2-weighted images are more sensitive to the WWPs. In Fig. 4B the WWPs appear dark because of a faster T_2-relaxation whereas the granules and void space are similar in signal intensity.

The WWPs show a similar behavior compared to the MCPs. An accumulation in the void space and around the granule surfaces is observed after both injections (see Fig. 4, steps II and III). Particles distribute within the granular sludge bed in the region of $x = 5–10$ mm and $z = 5–20$ mm. The granular sludge bed was slightly rearranged during both particle loadings as indicated in Fig. 4A, step I compared to II and III. In this case the particles were slightly pushed through the granular sludge bed. In Fig. 4, step III the additional particle load led to further infiltration of WWPs along the height of the granule bed as well as accumulation at the inlet ($z = 5$ mm, $x = 3–10$ mm).

3.4. Comparison of particle distribution

In this section, 3D MRI datasets from the end of each experiment are analyzed and compared. SPIONs (Experiment 1) and micro particles (Experiment 2 and 3) interact differently with the granular sludge bed (Fig. 5). The SPIONs penetrated into the granules and remained immobilized/sorbed (white bars, Fig. 5). Analysis of these 3D MRI datasets further revealed that SPIONs penetrated each granule independent of its surrounding environment (e.g., packaging density, granule size). Sorption of SPIONs occurred homogenously within the granular bed height ($z = 3–13$ mm) as presented in Fig. 6, Experiment 1. The penetration depth for SPIONs into the granules was estimated to up to 300±50μm.

Due to the flow direction that's compacting the granular sludge bed, the granule content in Experiment 1 is the highest ($\approx$60% for "granule" and "granule + particle") in Fig. 5. The higher flow velocity in Experiment 2 and the channeling event lead to a lower granule fraction compared to Experiment 3. In general, the "granule" fraction is underestimated within this approach, due to

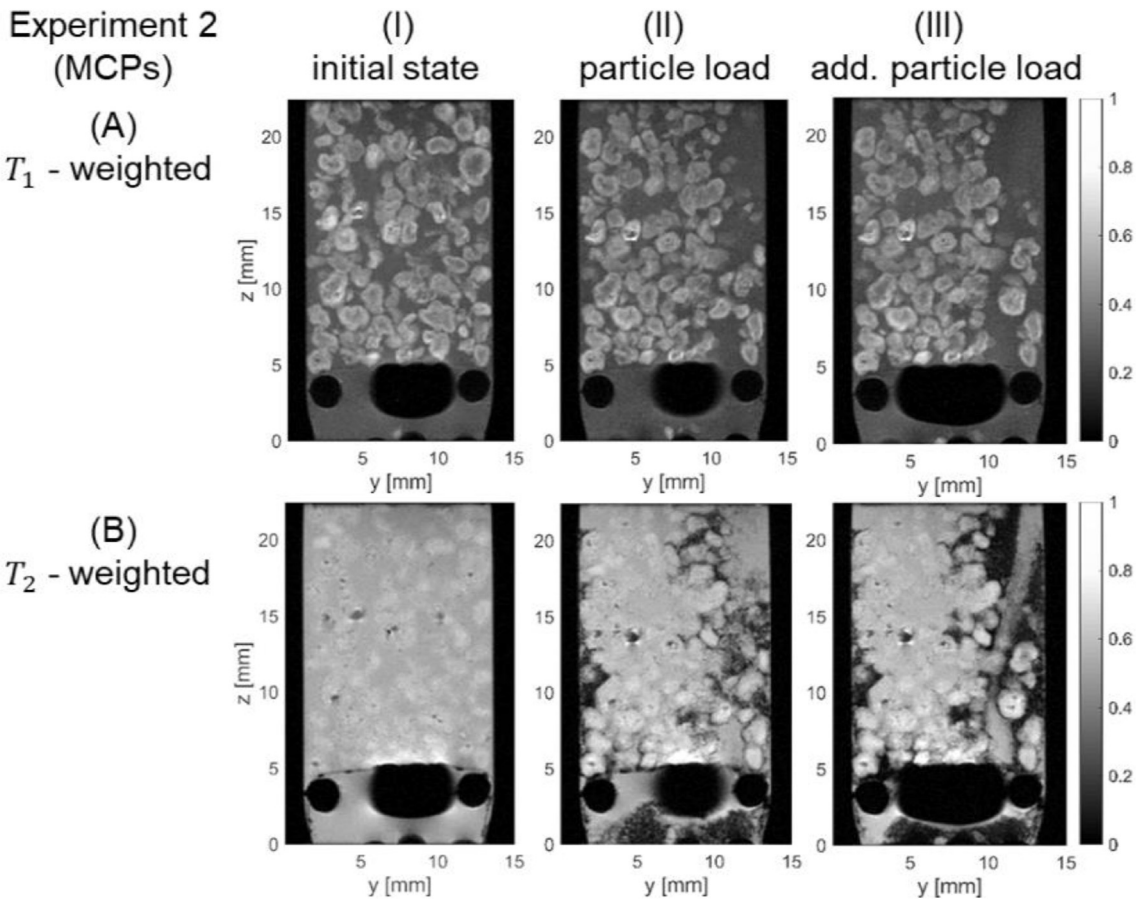

Fig. 3. 2D MRI images showing the accumulation of microcrystalline cellulose particles (MCPs) in the granular sludge bed. T_1-weighted images (A) allow for a differentiation between granules and water filled pore space, while T_2-weighted images (B) are more sensitive to the particle load in form of low intensity signals. The granule bed reordered during the particle load, and a flow channel formed. An accumulation of MCPs occurred mainly near the inlet and along the flow channel (preferential flow path).

lower signal intensities at the inner of the aerobic granules.

Compared to the behavior of SPIONs, MCPs locate nearby granules (see Fig. 5, Experiment 2) but do not penetrate the granules. In consequence, the fraction of "granule + particle" (white color allocation) is below 1% in Fig. 5 for MCPs compared to approximately 34% for SPIONs. Since the WWPs are larger than the MCPs no penetration of the larger particles into the granules is assumed. MCPs and WWPs behave similarly in terms of spatial distribution. Moreover, micro particles preferentially accumulate at lower parts of the granular sludge bed rather than distributing equally within the void space due to advective and diffusive transport processes as concluded from Fig. 6, Experiment 2 and 3. The distribution of MCPs is mainly affected by the geometry of the flow path (Fig. 6, Experiment 2). Particles gradually fill the void space along the channel, which causes a heterogeneous distribution of MCPs. In addition, a deposit of settled MCPs on top of the granular sludge bed was detected. The wastewater particle fraction (yellow) is sharply decreasing within the lower part ($z = 4$–6 mm) of the granule bed (see Fig. 6 Experiment 3). The low "particle" fraction for WWPs in Fig. 5, indicates that most particles are already retained at the glass spheres positioned below the granular sludge bed (Fig. 1). Almost complete particle retention was observed within the first 20 mm of the granule bed (see Fig. 6C, Experiment 3). Also, an additional particle load or a higher flow velocity would release particles to the bulk phase atop the granular sludge bed similar to the observations made in Experiment 2.

4. Discussion

4.1. Applicability of MRI

The results prove the applicability of MRI to study the fate and transport of particles into and through a settled bed of aerobic granules. T_1-weighted images were successfully applied to resolve the structure of a settled bed of aerobic granules. Colloidal (SPIONs) as well as micro particles (MCPs, WWPs) were resolved in time and space (x, y, z) by T_2-weighted images.

Further processing and merging of 3D MRI data sets allowed for the determination of the particle position inside the granular sludge bed. Some uncertainties remain in the predictability of the granule and void space volume fractions. Because of their signal intensity, the cores of the granules are assigned to the void space fraction. The changes in signal intensity caused by diverse relaxation times within biofilms are usually aligned with its properties (i.e. compactness and chemical composition). For example, Bartacek et al. (2016) observed that the outer zone of aerobic granules has a faster T_1 and T_2-relaxation than the inner core. The faster relaxation times might be related to a higher amount of extracellular polymeric substances (EPS) and microorganisms at the outer layers (Adav et al., 2008; McSwain et al., 2005; Wang et al., 2005). Further, the presence of precipitates in granules was reported, which locally fastened relaxation time (Herrling et al., 2017; Kirkland, 2017). Nevertheless, advanced image segmentation might improve the differentiation of void space and granule

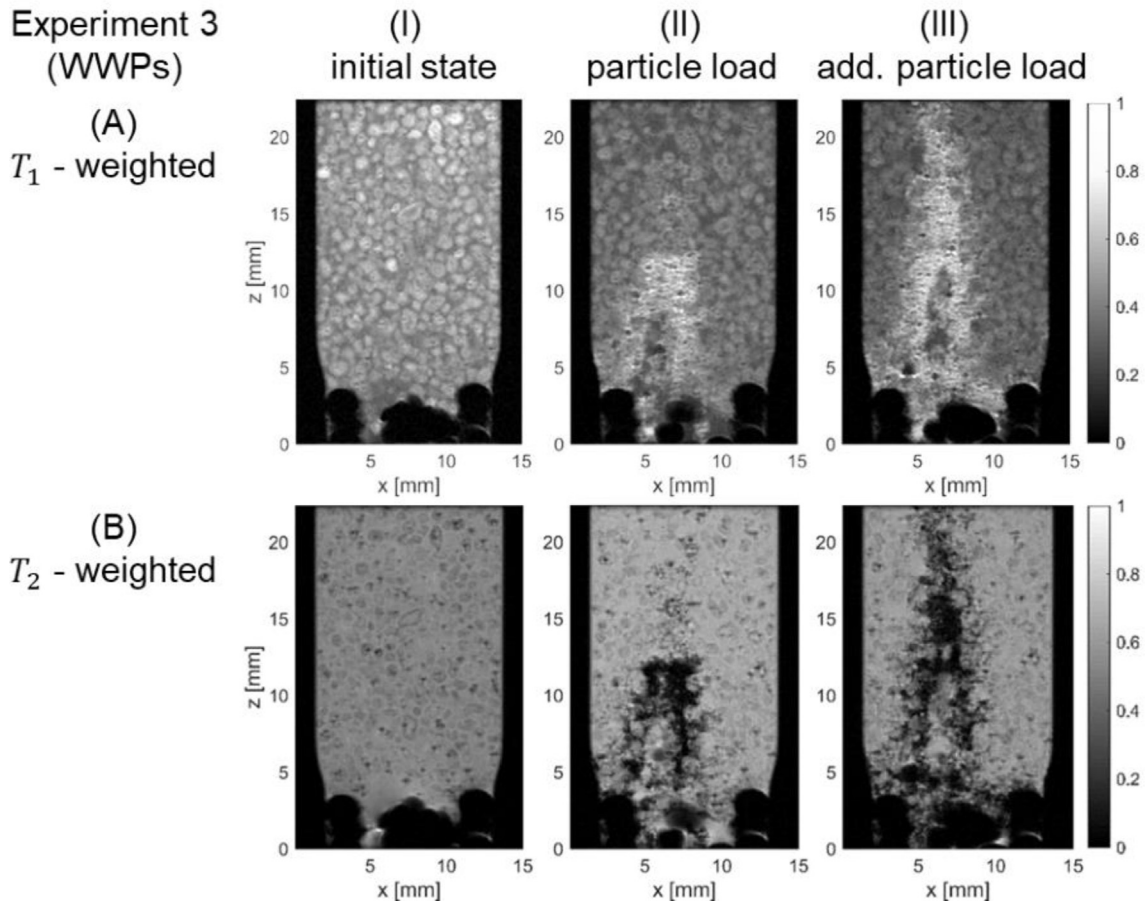

Fig. 4. 2D MRI images showing the accumulation of real wastewater particles (WWPs) within the granular sludge bed. In T_1-weighted images (A) granules, water filled pore space (low signal intensity) and particles (high signal intensity) are visible. The T_2-weighted images (B) display the particles more homogenously. Particles appear dark (low signal intensity) whereas the water filled pore space and granules appear grayish (high signal intensity). The particles accumulated mainly within a channeled void space of the granular sludge bed.

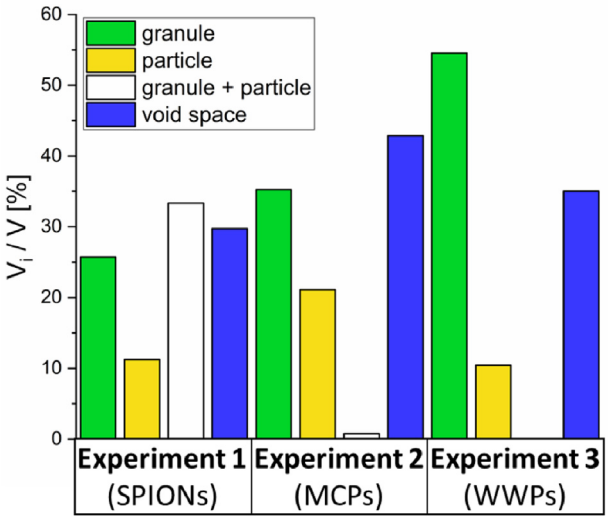

Fig. 5. Volume fractions at the end of each experiment. SPIONs are able to penetrate the granules (white bars), while the WWPs and MCPs accumulate in the void space.

core via shape validating tools as applied by Bégin et al. (2014) on nerve fibers.

4.2. Particle retention

The current study demonstrates that the retention mechanism of particulate organic matter is size dependent. Retention of particulate organic matter in an aerobic granular sludge reactor increases with decreasing influent wastewater particle size (Schwarzenbeck et al., 2004). Our results show that colloidal particles distribute equally within the granular sludge bed under applied flow. Thus, colloidal particles are able to attach and penetrate granules. We hypothesize that the hydrolysis of colloidal particles takes place within the granules and will lead to a rather uniform distribution of additional substrate during the subsequent cycles of a SBR. Furthermore, the estimated penetration depth up to $300 \pm 50\mu m$ suggests that the colloidal particles partially immobilize within the anoxic zone of aerobic granules. Therefore, hydrolysis would potentially release organic carbon to phosphorous accumulating and denitrifying microorganisms in the anoxic zone and contribute to the growth of stable and compact granules (de Kreuk and Van Loosdrecht, 2004; Layer et al., 2019; Pronk et al., 2015a).

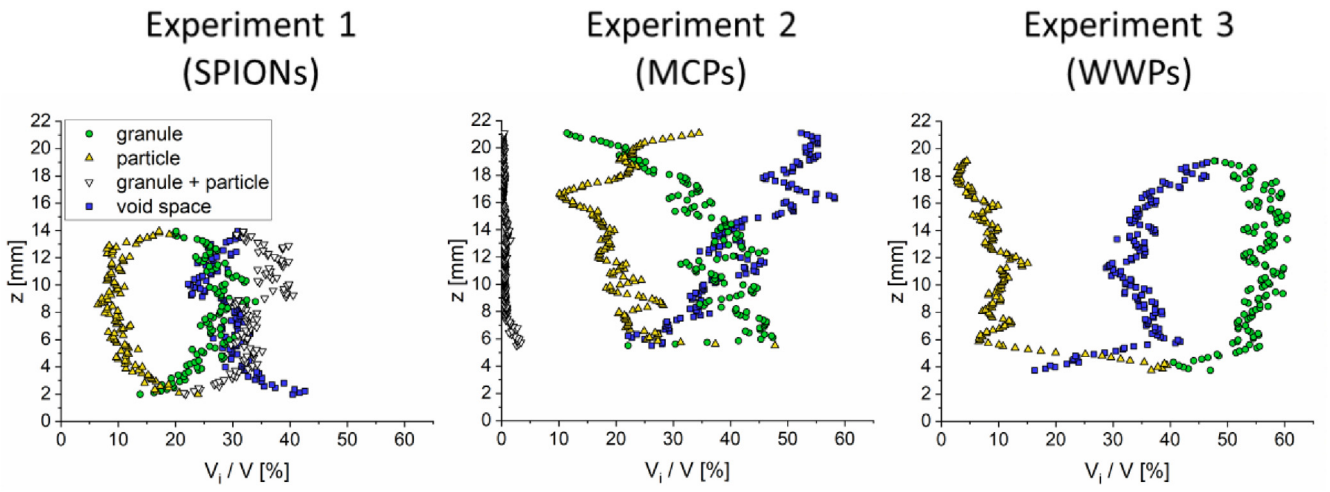

Fig. 6. Particle distribution along height. In Experiment 1 the SPIONs distributed homogenously along the height of the granular sludge bed. The accumulation of MCPs in Experiment 2 is mainly affected by the geometry of the flow path. The amount of accumulated WWPs in Experiment 3 decreases sharply within the first millimeters.

Experiments with MCPs and WWPs support findings of Schwarzenbeck et al. (2004) who concluded that the removal efficiency of micro particles seems critical. Recent studies demonstrated that micro particles are not able to penetrate granules and are retained at the granule surface (De Kreuk et al., 2010; Morgenroth et al., 2002; Pronk et al., 2015a; Wagner et al., 2015). This study supports and extends this knowledge, as the accumulation of micro particles inside the void space was directly visualized during the feeding phase. Further particle accumulation leads to the formation of particle layers. The particle layer thickness exceeds the particle diameter, which leads to the conclusion that most of the particles are not attached to the granule surface but remain available/mobile after the feeding phase. Overall, around 80% of the particulate organic matter are in the micrometer range after a primary treatment step (Sophonsiri and Morgenroth, 2004). Therefore, a large quantity of particulate organic matter might not necessarily be washed out with the effluent but stays distributed/remobilized over the whole reactor within the (aerobic) mixing phase.

4.3. Influence of flow velocity on particle distribution

Average flow velocity through the granular sludge bed during the anaerobic feeding phase is a particularly important strategic parameter. Experiment 1 showed that convection is necessary to distribute the SPIONs over the granular sludge bed. Here, a low flow velocity of 0.78 m/h allowed for a uniform distribution of particles within the void space, which is followed by sorption of SPIONs to aerobic granular sludge. The entire process resulted in an even distribution of SPIONs within the granular sludge bed. The impact of flow on the particle distribution is evident in the experiments utilizing MCPs and WWPs, respectively. Channels formed, that led to preferential flow and thus advective transport of particles occurred. In Experiment 2, high velocities inside the channel lead to a transport the MCPs through the entire granular sludge bed. This caused the sedimentation of MCPs on top of the granular sludge bed. In case of the WWPs a reduced average velocity of 0.39 m/h was sufficient to retain the majority of the particles within the first 20 mm of the settled bed of aerobic granules. However, for the typical anaerobic feeding time of around 1 h 0.39 m/h would be much too low. Typically, average flow velocities range from 1 to 5 m/h for low strength wastewater (Derlon et al., 2016; Li et al., 2014; Pronk et al., 2015b; Wagner et al., 2015). Channeling has been reported on full scale reactors at average filter velocities from 3 to 3.3 m/h (Pronk et al., 2015b). Our findings indicate that channeling might also occur at average filter velocities below 1 m/h. Hence, average filter velocities and volume exchange ratio should be considered to minimize the risk of washing out particulate organic matter during simultaneous fill and draw, as applied by Pronk et al. (2015b) on full scale reactors.

Conclusions

- MRI is a suitable analytical tool to visualize and quantify the transport and retention behavior of colloidal (SPIONs) and micro particles (microcrystalline cellulose particles (MCPs) and real wastewater particles (WWPs) inside a granular sludge bed. The combination of T_1- and T_2-weighted images allowed for the localization of granules, void space and particles in all spatial directions and over time.
- The size of particles (colloidal or several micrometer large) governs their fate within the granular sludge bed during feeding.
- Colloidal particles (SPIONs) distributed evenly over the granular sludge beds. These also penetrate the granules homogeneously by up to 300 ± 50 μm. As these particles are retained and immobilized inside the granules, degradation will most likely occur delivering additional substrate even in anoxic regions of aerobic granules.
- Micrometer-sized particles of micro crystalline cellulose (model particles) as well as real wastewater particles were affected by gravitation/sedimentation. Particles accumulated within as well as on top of the granular sludge bed. Results indicate that a large fraction of these particles remains mobile and might be degraded in subsequent phases of a SBR cycle or might be discharged causing constant or elevated effluent concentrations.

Declaration of competing interest

The authors declare that they have no known competing financial interests or personal relationships that could have appeared to influence the work reported in this paper.

Acknowledgements

The authors would like to thank the Karlsruhe Institute of Technology (KIT) for financial funding. DFG is acknowledged for financial support of the 200 MHz spectrometer. N. Schork and S.

Schuhmann are thanked for providing the Matlab scripts used for image processing.

Appendix A. Supplementary data

Supplementary data to this article can be found online at https://doi.org/10.1016/j.wroa.2020.100050.

References

Adav, S.S., Lee, D.-J., Tay, J.-H., 2008. Extracellular polymeric substances and structural stability of aerobic granule. Water Res. 42 (6–7), 1644–1650.

Bartacek, J., Vergeldt, F.J., Maca, J., Gerkema, E., Van As, H., Lens, P.N., 2016. Iron, cobalt, and gadolinium transport in methanogenic granules measured by 3D magnetic resonance imaging. Front. Environ. Sci. 4, 13.

Bégin, S., Dupont-Therrien, O., Bélanger, E., Daradich, A., Laffray, S., De Koninck, Y., Côté, D.C., 2014. Automated method for the segmentation and morphometry of nerve fibers in large-scale CARS images of spinal cord tissue. Biomed. Optic Express 5 (12), 4145.

Benneouala, M., Bareha, Y., Mengelle, E., Bounouba, M., Sperandio, M., Bessiere, Y., Paul, E., 2017. Hydrolysis of particulate settleable solids (PSS) in activated sludge is determined by the bacteria initially adsorbed in the sewage. Water Res. 125, 400–409.

Boltz, J.P., Motta, E.J.L., 2007. Kinetics of particulate organic matter removal as a response to bioflocculation in aerobic biofilm reactors. Water Environ. Res. 79 (7), 725–735.

Bouma, B., 2001. Handbook of Optical Coherence Tomography. CRC Press.

Confer, D.R., Logan, B.E., 1997. Molecular weight distribution of hydrolysis products during the biodegradation of model macromolecules in suspended and biofilm cultures. II. Dextran and dextrin. Water Res. 31 (9), 2137–2145.

Cuny, L., Herrling, M.P., Guthausen, G., Horn, H., Delay, M., 2015. Magnetic resonance imaging reveals detailed spatial and temporal distribution of iron-based nanoparticles transported through water-saturated porous media. J. Contam. Hydrol. 182, 51–62.

De Kreuk, M., Kishida, N., Tsuneda, S., Van Loosdrecht, M., 2010. Behavior of polymeric substrates in an aerobic granular sludge system. Water Res. 44 (20), 5929–5938.

de Kreuk, M.v., Van Loosdrecht, M., 2004. Selection of slow growing organisms as a means for improving aerobic granular sludge stability. Water Sci. Technol. 49 (11–12), 9–17.

Derlon, N., Wagner, J., da Costa, R.H.R., Morgenroth, E., 2016. Formation of aerobic granules for the treatment of real and low-strength municipal wastewater using a sequencing batch reactor operated at constant volume. Water Res. 105, 341–350.

Giesen, A., De Bruin, L., Niermans, R., Van der Roest, H., 2013. Advancements in the application of aerobic granular biomass technology for sustainable treatment of wastewater. Water Pract. Technol. 8 (1), 47–54.

Graf von der Schulenburg, D., Akpa, B., Gladden, L., Johns, M., 2008. Non-invasive mass transfer measurements in complex biofilm-coated structures. Biotechnol. Bioeng. 101 (3), 602–608.

HaskoningDHV, R., 2020. A to Z NEREDA® Plants.

Herrling, M.P., Lackner, S., Nirschl, H., Horn, H., Guthausen, G., 2019. Recent NMR/MRI studies of biofilm structures and dynamics. Annu. Rep. NMR Spectrosc. 97, 163.

Herrling, M.P., Weisbrodt, J., Kirkland, C.M., Williamson, N.H., Lackner, S., Codd, S.L., Seymour, J.D., Guthausen, G., Horn, H., 2017. NMR investigation of water diffusion in different biofilm structures. Biotechnol. Bioeng. 114 (12), 2857–2867.

Kirkland, C.M., 2017. Nuclear Magnetic Resonance Studies of Biofilm-Porous Media Systems. Montana State University-Bozeman, College of Engineering.

Layer, M., Adler, A., Reynaert, E., Hernandez, A., Pagni, M., Morgenroth, E., Holliger, C., Derlon, N., 2019. Organic substrate diffusibility governs microbial community composition, nutrient removal performance and kinetics of granulation of aerobic granular sludge. Water Res. X 4, 100033.

Li, C., Brunner, F., Wagner, M., Lackner, S., Horn, H., 2018. Quantification of particulate matter attached to the bulk-biofilm interface and its influence on local mass transfer. Separ. Purif. Technol. 197, 86–94.

Li, J., Ding, L.-B., Cai, A., Huang, G.-X., Horn, H., 2014. Aerobic sludge granulation in a full-scale sequencing batch reactor. BioMed Res. Int. 2014, 12. https://doi.org/10.1155/2014/268789, 2014, 268789.

Manz, B., Volke, F., Goll, D., Horn, H., 2003. Measuring local flow velocities and biofilm structure in biofilm systems with magnetic resonance imaging (MRI). Biotechnol. Bioeng. 84 (4), 424–432.

McSwain, B., Irvine, R., Hausner, M., Wilderer, P., 2005. Composition and distribution of extracellular polymeric substances in aerobic flocs and granular sludge. Appl. Environ. Microbiol. 71 (2), 1051–1057.

Morgenroth, E., Kommedal, R., Harremoës, P., 2002. Processes and modeling of hydrolysis of particulate organic matter in aerobic wastewater treatment–a review. Water Sci. Technol. 45 (6), 25–40.

Neu, T.R., Manz, B., Volke, F., Dynes, J.J., Hitchcock, A.P., Lawrence, J.R., 2010. Advanced imaging techniques for assessment of structure, composition and function in biofilm systems. FEMS Microbiol. Ecol. 72 (1), 1–21.

Orhon, D., Çokgör, E.U., 1997. COD fractionation in wastewater characterization—the state of the art. J. Chem. Technol. Biotechnol.: Int. Res. Process Environ. Clean Technol. 68 (3), 283–293.

Peszynska, M., Trykozko, A., Iltis, G., Schlueter, S., Wildenschild, D., 2016. Biofilm growth in porous media: experiments, computational modeling at the porescale, and upscaling. Adv. Water Resour. 95, 288–301.

Phoenix, V., Holmes, W., Ramanan, B., 2008. Magnetic resonance imaging (MRI) of heavy-metal transport and fate in an artificial biofilm. Mineral. Mag. 72 (1), 483–486.

Pronk, M., Abbas, B., Al-Zuhairy, S., Kraan, R., Kleerebezem, R., Van Loosdrecht, M., 2015a. Effect and behaviour of different substrates in relation to the formation of aerobic granular sludge. Appl. Microbiol. Biotechnol. 99 (12), 5257–5268.

Pronk, M., De Kreuk, M., De Bruin, B., Kamminga, P., Kleerebezem, R.v., Van Loosdrecht, M., 2015b. Full scale performance of the aerobic granular sludge process for sewage treatment. Water Res. 84, 207–217.

Ramanan, B., Holmes, W.M., Sloan, W.T., Phoenix, V.R., 2013. Magnetic resonance imaging of mass transport and structure inside a phototrophic biofilm. Curr. Microbiol. 66 (5), 456–461.

Ranzinger, F., Herrling, M.P., Lackner, S., Grande, V.W., Baniodeh, A., Powell, A.K., Horn, H., Guthausen, G., 2016. Direct surface visualization of biofilms with high spin coordination clusters using magnetic resonance imaging. Acta Biomater. 31, 167–177.

Rocktäschel, T., Klarmann, C., Ochoa, J., Boisson, P., Sørensen, K., Horn, H., 2015. Influence of the granulation grade on the concentration of suspended solids in the effluent of a pilot scale sequencing batch reactor operated with aerobic granular sludge. Separ. Purif. Technol. 142, 234–241.

Ruiken, C., Breuer, G., Klaversma, E., Santiago, T., Van Loosdrecht, M., 2013. Sieving wastewater—Cellulose recovery, economic and energy evaluation. Water Res. 47 (1), 43–48.

Schwarzenbeck, N., Erley, R., Wilderer, P., 2004. Aerobic granular sludge in an SBR-system treating wastewater rich in particulate matter. Water Sci. Technol. 49 (11–12), 41–46.

Seymour, J.D., Gage, J.P., Codd, S.L., Gerlach, R., 2004. Anomalous fluid transport in porous media induced by biofilm growth. Phys. Rev. Lett. 93 (19), 198103.

Sophonsiri, C., Morgenroth, E., 2004. Chemical composition associated with different particle size fractions in municipal, industrial, and agricultural wastewaters. Chemosphere 55 (5), 691–703.

Wagner, J., Weissbrodt, D.G., Manguin, V., da Costa, R.H.R., Morgenroth, E., Derlon, N., 2015. Effect of particulate organic substrate on aerobic granulation and operating conditions of sequencing batch reactors. Water Res. 85, 158–166.

Wagner, M., Manz, B., Volke, F., Neu, T.R., Horn, H., 2010. Online assessment of biofilm development, sloughing and forced detachment in tube reactor by means of magnetic resonance microscopy. Biotechnol. Bioeng. 107 (1), 172–181.

Wang, Z.-W., Liu, Y., Tay, J.-H., 2005. Distribution of EPS and cell surface hydrophobicity in aerobic granules. Appl. Microbiol. Biotechnol. 69 (4), 469.

Wilén, B.-M., Liébana, R., Persson, F., Modin, O., Hermansson, M., 2018. The mechanisms of granulation of activated sludge in wastewater treatment, its optimization, and impact on effluent quality. Appl. Microbiol. Biotechnol. 102 (12), 5005–5020.